Paper ID ICLASS06-074
EVALUATION OF IN-CYLINDER FLOW STRUCTURES AND GDI SPRAY PROPAGATION OVER A RANGE OF ENGINE SPEEDS AND INJECTION TIMING

P. Stansfield[1], G. Wigley[1], G. Pitcher[2] and H. Nuglisch[3]

[1] Aeronautical and Automotive Engineering, Loughborough University, Leicestershire, LE11 3TU, UK. G.Wigley@Lboro.ac.uk
[2] Powertrain Research, Lotus Engineering Ltd, Hethel, Norwich, NR14 8EZ, UK, GPitcher@Lotuscars.co.uk
[3]Siemens VDO Automotive S.A.S., 31036 Toulouse, France, Hans.Nuglish@Siemens.com

ABSTRACT The in-cylinder flow field during the latter half of the intake stroke in a single cylinder optical engine operating at 750, 2000 and 3500 rpm has been quantified by PIV. This was complemented by a Mie imaging study of the structure of multi-stream GDI sprays with injection timings of 90 120 and 150 ^{0}CA. The vector fields and spray images at specific crankangles have been used to demonstrate the effect of inlet air velocity on the disruption and transport of the fuel spray. The study has shown that it is the early airflow through the valve gap that is more responsible for fuel disruption than the latter air motion.

Keywords: GDI, PIV, Mie Imaging, Fuel spray, Flow structures.

1. INTRODUCTION

The most fuel efficient way of operating a gasoline internal combustion (IC) engine is to burn the fuel in excess air. However, in homogeneous IC engines, as the air-fuel ratio is increased, the flame speed reduces until combustion limits are reached. To maintain combustible air-fuel ratios, port fuelled engines have incorporated a throttle to regulate the mass of inducted air. The pumping losses associated with drawing air past this restriction significantly reduces the maximum fuel efficiency of port fuelled engines operating at part load [1].

Stratified Gasoline Direct Injection (GDI) has been proposed as one method of eliminating the pumping losses associated with throttling the intake flow. The first generation used a combination of shaped intake ports and piston crowns to generate airflow structures which transport the fuel spray towards the spark plug in order to create a kernel of a stoichiometric, or rich, mixture at the plug, while the extremities of the cylinder remain lean. The control of very small injected quantities without over-mixing is very difficult. The second generation of stratified DI engines use a spray guided system creating the stratification directly by a small quantity of injected fuel and igniting the mixture in the close vicinity of the spray[2]. The strong stratification allows a full, unthrottled, intake charge to be drawn on the intake stroke. The engine load is thereby controlled by the mass of fuel injected. GDI also offers benefits under full load conditions as the latent energy for fuel evaporation is drawn from the surrounding charge. The corresponding reduction in inlet temperature increases the volumetric efficiency of the engine and allows the compression ratio to be increased by 1 to 1.5 ratios[3].

While stratified GDI engines have shown significant savings in brake fuel consumption[4], concerns have been raised with regard to their emissions[5]. Locally rich areas of combustion have led to high emissions of sub-micron particulate matter and locally lean areas of combustion have produced high emissions of NOX. The development of catalytic de-NOX devices to reduce NOX emissions below the levels regulated by ULEV and EURO IV legislation have been shown to be poisoned by sulphur contents greater than 10 ppm in the fuel. At present, the majority of US and European gasoline fuel specifications do not meet this 10 ppm sulphur requirement.

It has recently been proposed that the emissions concerns of first generation GDI engines can be overcome by operating the engine with a homogeneous charge and stoichiometric conditions throughout the load speed range, with the air fuel mixing and combustion processes controlled by a fully variable valve train[6, 1]. Such an engine would be controlled by the mass of air inducted. This type of engine would retain the advantages of charge cooling and throttle-less operation, but would eliminate the high emissions of particulate matter. Furthermore, it could be fitted with a standard 3-way catalyst. A fully variable valve train would offer the potential for further benefits, such as cylinder or valve deactivation.

The reduction in mixing time between injection and ignition, requires that the quality of atomization from the injector nozzle and the ability of the airflow structures to break up and mix the spray plume are critical to the performance of a homogeneous GDI engine. In addition, impingement of the fuel spray onto the surfaces of the cylinder should be avoided to prevent liquid fuel films on the piston crown and oil dilution on the cylinder walls[7].

As such, the development of homogeneous GDI engines requires a precise knowledge of the transport and mixing of the liquid fuel, fuel vapour and air flow occurring within the cylinder over the intake and compression stroke. Optical diagnostic techniques, which do not perturb the flow, have been of considerable use for quantifying flow parameters and visualizing spray phenomena.

This paper discusses the use of the Particle Image Velocimetry (PIV) technique to characterize the airflow in the tumble plane within the cylinder of an optical research engine at speeds of 750, 2000 and 3,500 rpm. To complement this a MIE imaging study has also been performed to assess the interaction between the fuel sprays from a GDI multi-stream injector, with injection timings of 90^0, 120^0 and 150^0 ATDC inlet, and the airflow structures and impingement of the streams on the piston crown.

2. EXPERIMENTAL FACILITIES

2.1 Optically Accessed Engine

The Single Cylinder Optical Research Engine (SCORE), has been designed by Lotus Engineering specifically for the application of optical diagnostic techniques. The engine, shown in Figure 1, incorporates a full length fused silica liner and a sapphire window in the piston crown to provide extensive optical access to the combustion chamber. The piston contains a carbon fibre piston ring which runs in the optical liner to maintain correct compression pressures. The engine specifications are in Table 1. The engine has both primary and secondary balance shafts to allow for operation at speeds up to 5000 rpm. Engine timing data is provided by two optical encoders with 0.2° resolution, one of which is mounted on the end of the crankshaft and the other on a 2:1 drive to represent the camshaft.

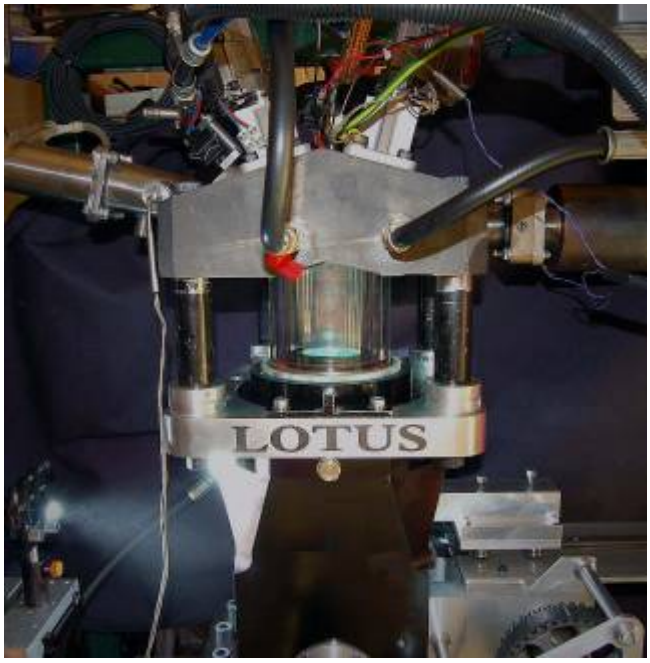

Fig. 1: SCORE

The overhead poppet valves are actuated by means of a fully variable electro-hydraulic valve system, the Lotus Active Valve Train, which allows complete control of the individual valve profiles. The engine and valve profile specifications for this work are given in Table 1. The valve timing is given relative to TDC valve overlap.

The engine contains a centrally mounted multistream gasoline fuel injector from Siemens VDO Automotive. The injector is fed 95 RON gasoline at 120 bar line pressure by a three cylinder gasoline fuel pump. This, in turn, is fed by a standard automotive fuel pump operating at 3.5 bar pressure. The injector contains five equally spaced orifices around a sixth central orifice. The fuel delivery axis was bent away from the injector axis by approximately 7.5° to allow for the mounting angle in the cylinder head and to avoid spray impingement on the inlet valves. The electronic control signals to the injector driver were generated by an AVL 4210 engine timing unit which was triggered by the optical encoders on the engine crankshaft and the 2:1 drive shaft.

Table 1: Engine Specification

Bore	88.0	mm
Stroke	82.1	mm
Capacity	0.50	L
Maximum Speed	5000	rpm
Compression Ratio	10:1	
Peak Compression Pressure	25	bar
Peak Compression (750 rpm)	19.2	bar
Peak Compression (2000 rpm)	22.1	bar
Peak Compression (3500 rpm)	22.0	bar

Valve Timing Data

IVO	675°	IVC	264°
EVO	462°	EVC	45°
Max. Inlet Lift	9.35 mm	Max. Exh. Lift	9.35 mm

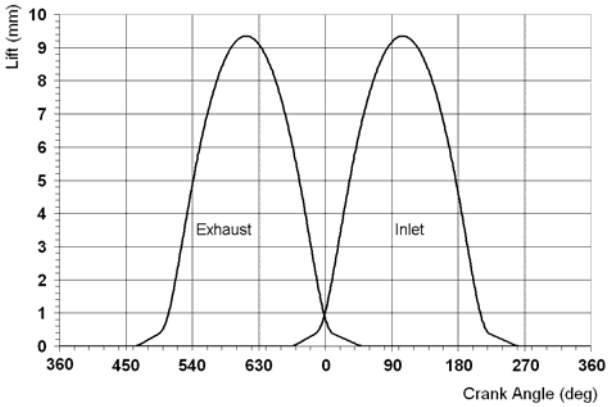

3. EXPERIMENTAL PROCEDURE

This paper discusses the PIV technique to measure the in-cylinder airflow under motored engine conditions, and, in a complementary experiment, the use of the Mie imaging technique to visualize the affect of these airflow structures on the development and propagation of the liquid fraction of the GDI fuel spray.

Both the PIV and Mie imaging experiments were performed at engine speeds of 750, 2000 and 3500 rpm. The Mie imaging was performed for injection timings of 90^0, 120° and 150° crank angle after TDC gas exchange. The crankangle window over which imaging was performed varied with engine speed but covered from 90^0 to over 270^0 ATDC.

3.1 Particle Image Velocimetry

A “Solo 120” Nd:YAG double pulsed laser was frequency doubled to produce co-linear beams of 512 nm wavelength which were directed at the 45° mirror in the extended crankcase then up through the sapphire window in the piston crown. The laser beam was expanded by means of a divergent cylindrical lens of focal length -20 mm. The resultant light sheet illuminated the cylinder in the vertical symmetry plane between the two inlet valves.

Silicon oil droplets of approximately 1μm diameter were fed into the intake ports by a La Vision seeding unit operating at nominally 2 bar. The droplets moving through the light sheets were imaged by a La Vision Flowmaster 3 fast shutter CCD camera fitted with a Nikon 60 mm Macro lens at f#11.3. The camera imaged an area of approximately 42 by 33.6 mm represented by 1280 by 1024 pixels. The imaged area was centrally located about the cylinder axis

and located in the vertical plane so as not to generate flare from the valves at maximum lift.

The main focus of the paper is the evaluation of how the in-cylinder flow structures at different engine speeds effect the propagation of the GDI spray. The PIV analysis therefore was only to cover the period of injection and mixing. As this period was fixed, up to 5 ms, the PIV image pair times, which were crank angle resolved, were selected to maintain an acceptable experimental run time, hence the PIV resolution had to be varied with engine speed. The PIV image capture settings are shown in Table 2.

The Laser was operated at approximately 500mj per pulse while the delay between pulses, Δt, was varied according engine speed. The air pressure to the seeder was finely adjusted until approximately 8-12 seeding particles could be seen in a typical 64 px by 64 px interrogation region of an image. Fifty one image pairs were captured at each crank angle to allow both mean flow fields and cycle to cycle variation to be analyzed.

Table 2: PIV Image times

RPM	Crank period	Resolution	Image Pairs	Δt
750	89.6°→169.6°	1.6°	51	70 μs
2000	88.8°→208.8°	2.4°	51	25 μs
3500	88.0°→248.0°	3.2°	51	15 μs

La Vision's "DaVis 7.0" PIV software was used to produce the vector plots. A multipass cross correlation algorithm was undertaken. The first pass employed a 128 px by 128 px interrogation area with 50% overlap. The second pass utilized a 64 px by 64 px interrogation area also with 50% overlap. The resulting vector field plots were therefore produced at 32 px by 32 px resolution.

No preprocessing of the raw images was applied. However, validation of the calculated vectors was undertaken by use of a variety of post processing techniques. A minimum signal to noise ratio of 1.5 was necessary to accept the vector and the flow continuity principle was applied to remove vectors which varied by more than 3 times the RMS value of their 8 surrounding neighbours. Finally, interrogation regions with fewer than four particle images were also rejected. A mean vector field was then calculated from all 51 cyclic results produced for each result.

3.2 Mie Imaging

The complementary imaging experiment was performed on the full bore and stroke of the engine, representing an imaged area of 112 by 90 mm. Illumination was provided by an EG&G xenon flash lamp connected to a Fostec fiber optic cable directed up into the cylinder by the 45° mirror. The engine was motored under identical conditions to the PIV experiment except that during this experiment the fuel injection system was activated.

The AVL timing unit was set to deliver an injection duration pulse of 2 ms. The injector driver incorporated a 1ms delay period between the start of the energizing pulse and the time at which the needle lifted and fuel began to leave the injector. As such, the injection timing relative to the engine crankangle had to be compensated for the delay so that fuel began to leave the injector at 90°, 120° and 150° after TDC gas exchange at all engine speeds. The fuel delivery time was 1ms.

The light scattered by the fuel droplets was collected by the same Flowmaster 3 camera and lens system as used in the PIV experiment. The exposure time of the camera was set to 2 μs and the f-number of the camera was set to f#5.6. A secondary flash was directed towards the cylinder head to provide background lighting to visualize the cylinder features. An 8 μs delay was incorporated between the flash signal and the camera shutter opening to maximize the captured light intensity.

Five images were taken at each crankangle to allow mean images of the spray to be presented. The images were processed on a grayscale background between 0→512 intensity counts. As the imaged area of the PIV experiment was smaller than the spray images then, in the spray images presented, the area covered by the PIV data is marked.

Imaging times were chosen so as to cover the injection event and mixing stages. The crankangle resolution was again altered with engine speed to maintain acceptable engine run times.

Table 3: Mie Image times

RPM	SOI	Crank period	Res^n	Scan Time
750	90°	89.6°→109.6°	0.2°	4.44ms
750	120°	119.6°→139.6°	0.2°	4.44ms
750	150°	149.6°→169.6°	0.2°	4.44ms
2000	90°	88.8°→148.8°	0.6°	5.00ms
2000	120°	118.8°→178.8°	0.6°	5.00ms
2000	150°	148.8°→208.8°	0.6°	5.00ms
3500	90°	88.0°→188.0°	1.0°	4.76ms
3500	120°	117.2°→257.2°	1.0°	4.76ms
3500	150°	147.2°→287.2°	1.0°	4.76ms

Injection Pulse = 2.0ms

3.3 Engine Simulation model

The engine geometry of the engine was entered into the 1D simulation code, "Lotus Engine Simulation" (LES). The calorific value of the fuel was set to 0.1KJ/Kg to represent motored conditions. The software code was run at the given engine speeds to provide instantaneous in cylinder conditions and air mass flow data into the cylinder. Selected results from the simulation at crank angles which correspond to the PIV vector fields are shown in Table 4.

Table 4: LES Simulation Results

RPM	Crank Angle	Mass flow rate kgs^{-1}	Cylinder Pressure bar
750	96.0°	0.023	1.00
2000	108.0°	0.085	0.92
3500	120.0°	0.045	0.92
750	128.0°	0.014	1.01
2000	139.2°	0.045	0.92
3500	152.0°	0.030	0.97
750	156.8°	0.006	1.00
2000	170.4°	0.021	0.94
3500	180.4°	0.010	1.03

4 RESULTS AND DISCUSSION

Three series of spray images and PIV flow maps are presented, in 4.1, 4.2 and 4.3 which correspond to fuel delivery beginning at 90°, 120° and 150° after TDC. The images shown occur after the end of injection and show the fuel spray detached from the nozzle when the fuel transport is solely effected by the airflow structures within the cylinder. The bulk of the fuel spray can be seen within the PIV measurement area.

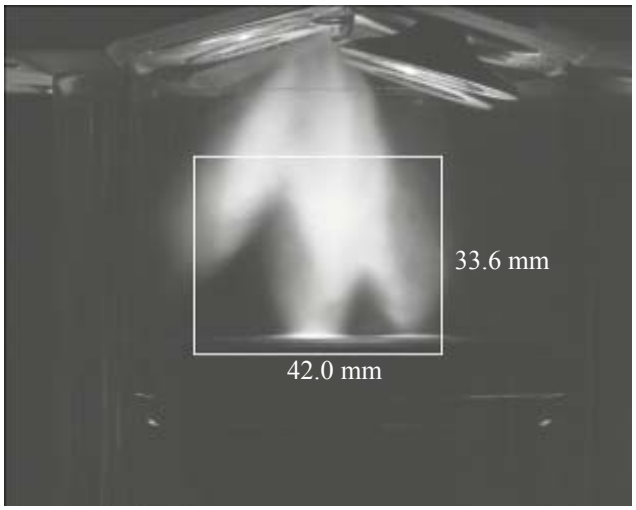

Crank Angle: 96.0° ATDC 750 rpm
Time After Start of injection: 1.33 ms

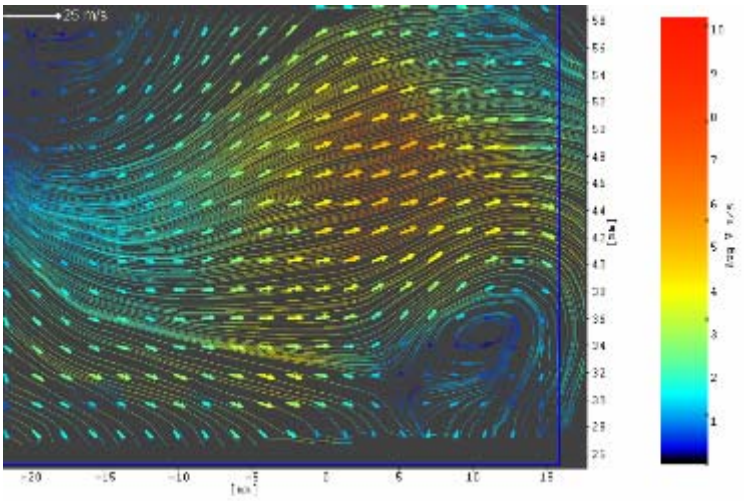

Velocity Range: 0 → 10 ms^{-1}

Crank Angle: 108.0° ATDC 2000 rpm
Time After Start of injection: 1.50 ms

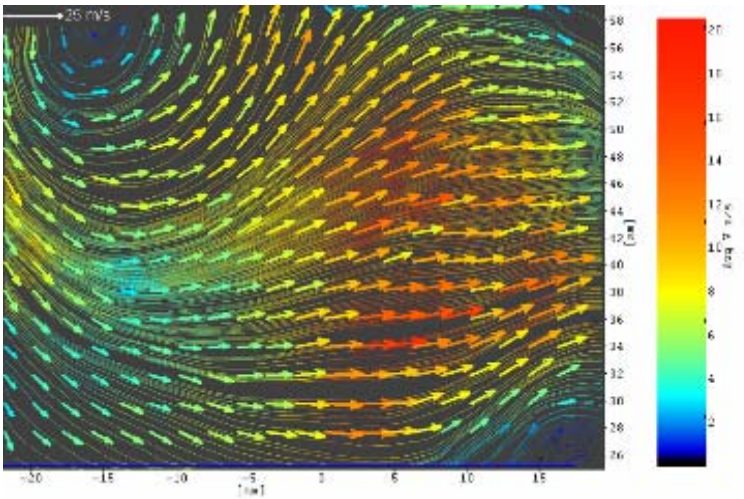

Velocity Range: 0 → 20 ms^{-1}

Crank Angle: 120.0° ATDC 3500rpm
Time After Start of injection: 1.42 ms

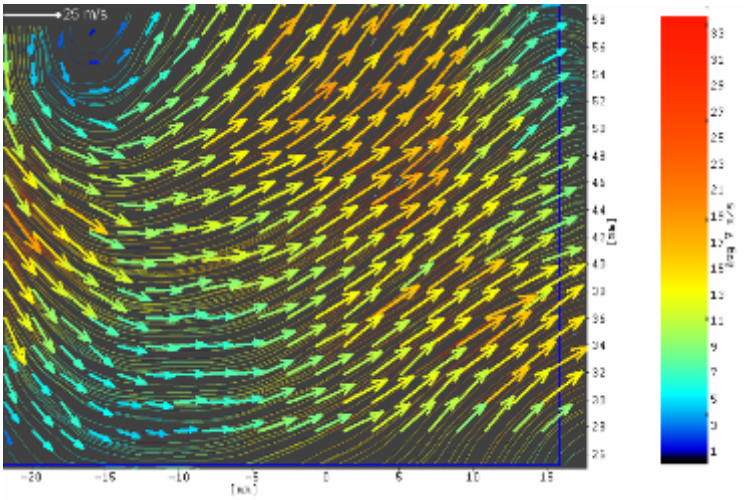

Velocity Range: 0 → 35 ms^{-1}

Fig. 4.1: Spray images and PIV maps – SOI 90^0

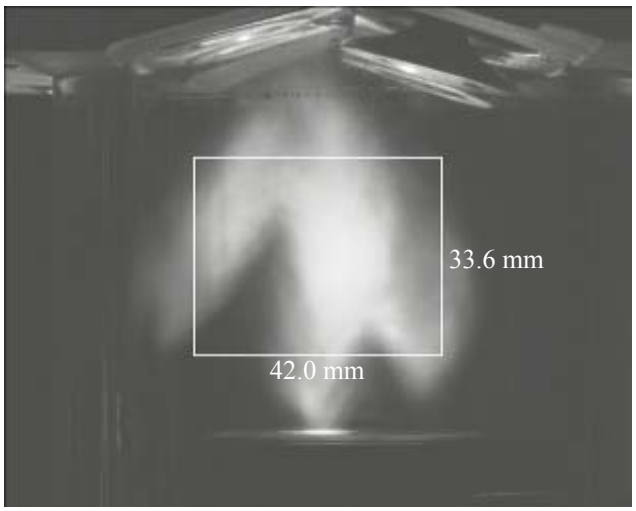

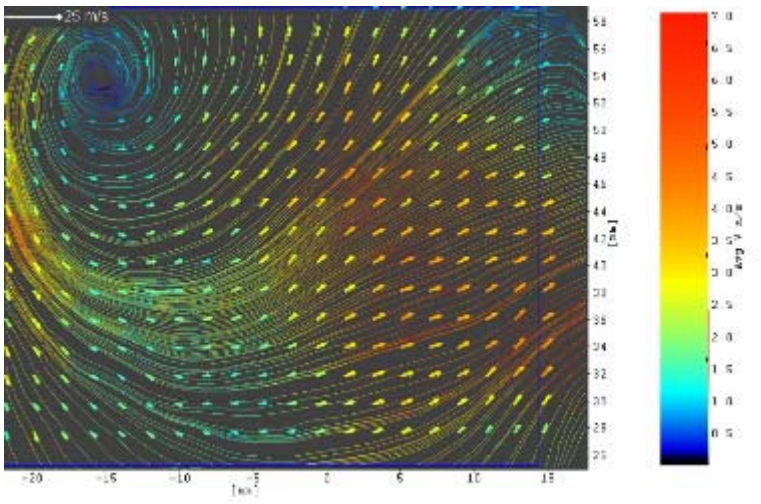

Crank Angle: 128.0° ATDC 750 rpm
Time After Start of injection: 1.78 ms

Velocity Range: 0 → 7 ms^{-1}

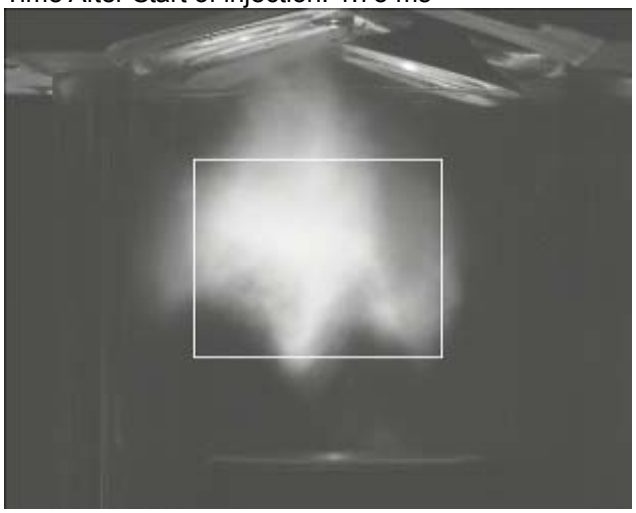

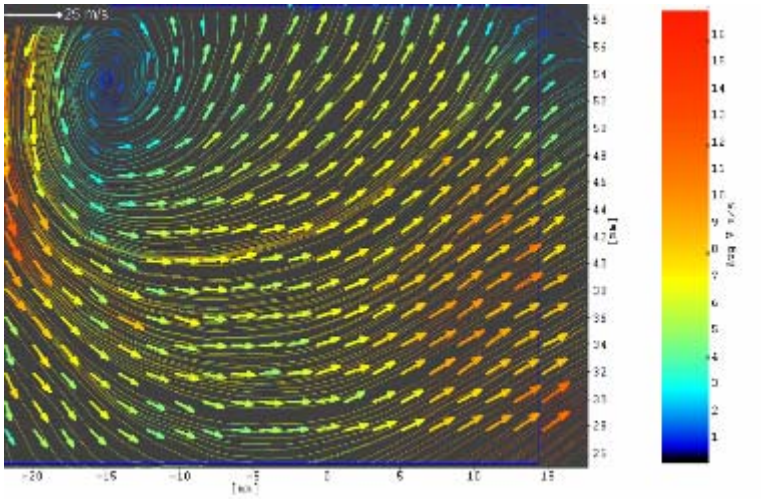

Crank Angle: 139.2° ATDC 2000 rpm
Time After Start of injection: 1.60 ms

Velocity Range: 0 → 18 ms^{-1}

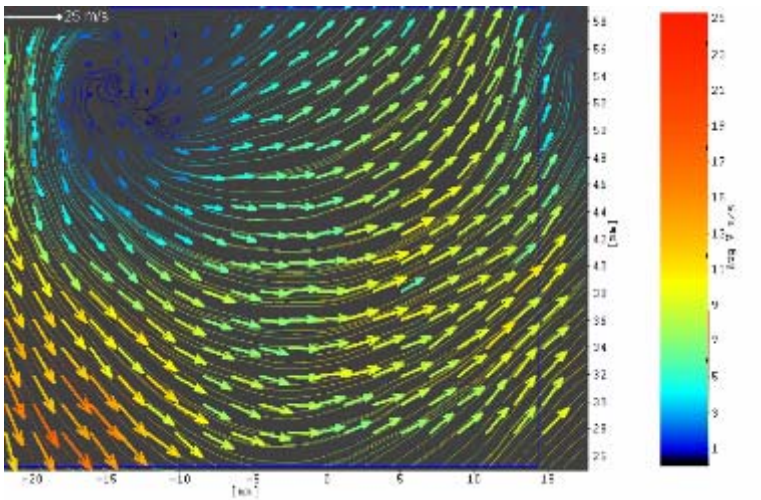

Crank Angle: 152.0° ATDC 3500rpm
Time After Start of injection: 1.52 ms

Velocity Range: 0 → 25 ms^{-1}

Fig. 4.2: Spray images and PIV maps – SOI 120^0

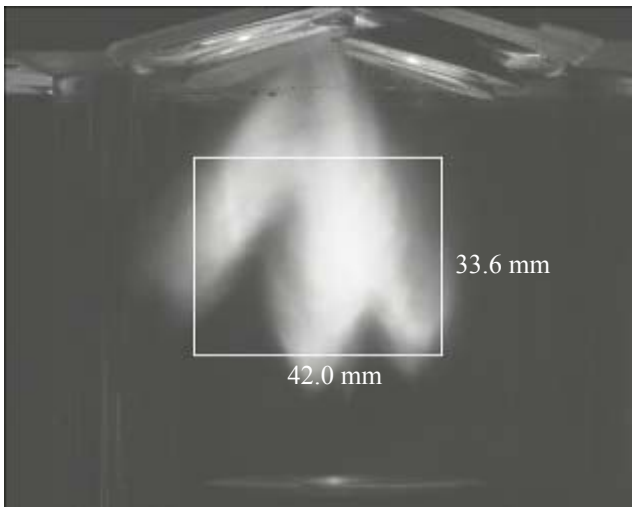

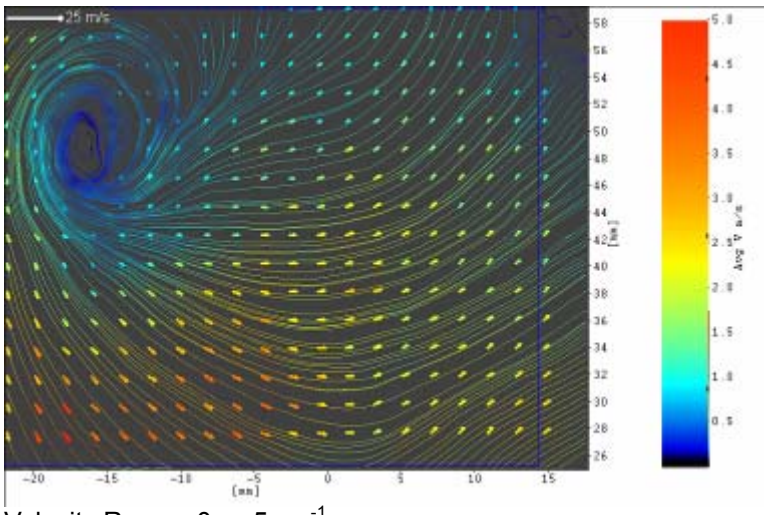

Crank Angle: 156.8° ATDC 750 rpm
Time After Start of injection: 1.51 ms

Velocity Range: 0 → 5 ms^{-1}

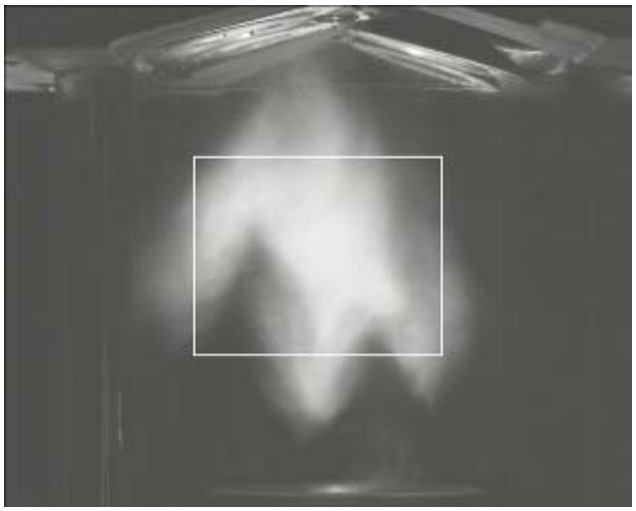

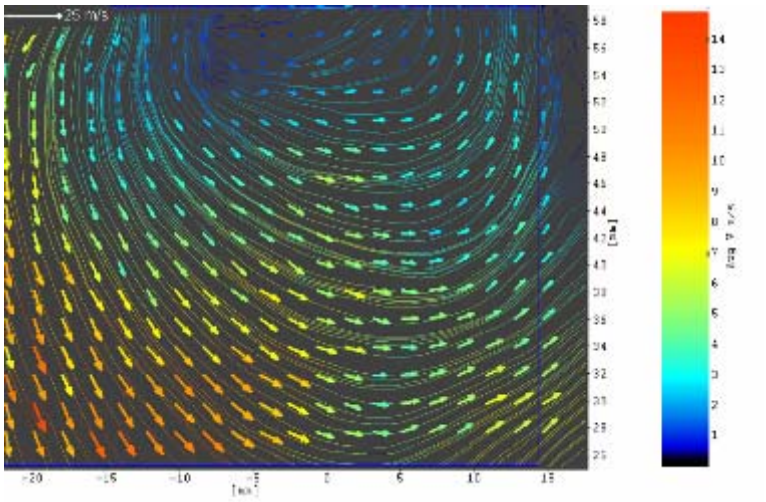

Crank Angle: 170.4° ATDC 2000 rpm
Time After Start of injection: 1.70 ms

Velocity Range: 0 → 15 ms^{-1}

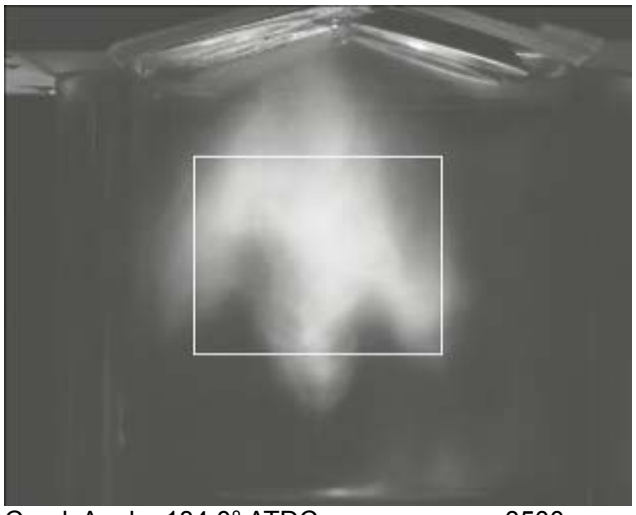

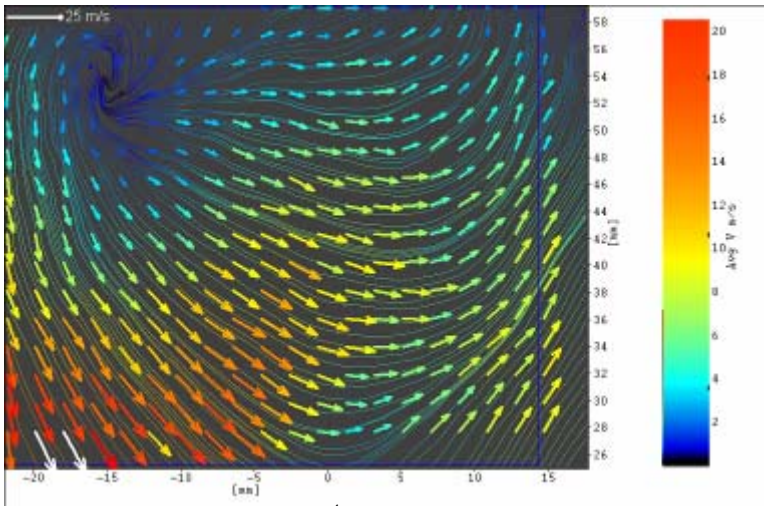

Crank Angle: 184.0° ATDC 3500rpm
Time After Start of injection: 1.61 ms

Velocity Range: 0 → 20 ms^{-1}

Fig. 4.3: Spray images and PIV maps – SOI - 150^0

Mie images at various times between 1.33 ms and 1.78 ms after the start of injection are shown in Figures 4.1, 4.2 and 4.3. The corresponding flow fields produced under each engine condition are presented alongside. Streamlines, calculated from the vector fields, have been plotted to indicate the tumble nature of the flow. A constant reference vector length of 25 ms^{-1} is shown in the top left corner of each vector field. The vector colour coding scheme has, however, been re-scaled for each vector field to best represent the wide range of velocities produced at the various engine speeds and crankangles

The mean flow structures show that the overriding feature of the flow in this symmetry plane is the development of an anti-clockwise tumble motion with the inlet air moving down the liner on the left under the exhaust valves then across the liner above the piston which is then directed up towards the inlet valves in the top right.

Two recirculation zones can be identified. The first recirculation, found in the upper left hand corner of the image, is common to all of the PIV flow fields and is caused by the majority of flow directed by the inlet manifold over the top of the inlet valves and then being forced to turn towards the piston crown by the cylinder walls. The location of the recirculation remains relatively stable during the majority of the intake stroke. A second recirculation can be seen near the lower right hand corner of the PIV region in Figure 4.1, i.e. for injection at 90^0 ATDC. Later PIV flow fields show that this recirculation follows the piston as it descends during the remainder of the intake stroke.

As the start of injection is retarded from 90° to 150° ATDC, the magnitude of the vector scale is reduced, in the case of the 3500 rpm engine speed the peak scale velocities range from 33ms^{-1} at 90°, to 25 ms^{-1} at 120^0CA and then to 20 ms^{-1} at 150°. To quantify the overall variation in flow velocity as a function of engine speed the radial velocity component down the cylinder centreline is plotted in Figure 5 for the crankangle 120^0, i.e. corresponding to highest velocities recorded in the PIV interrogation area. The vertical scale has 0 mm referenced to the piston crown at BDC.

A comparison between the spray in the engine at 750 rpm and the spray produced under atmospheric conditions by an identical injector is shown in Figure 6. The orientation of the injectors to the camera was identical in each case and the images times corresponded to 1 ms after fuel appeared at the nozzle. Each image shows two overlapping streams on the left hand side, a single stream on the far right and three streams nearly superimposed down the vertical axis through the injector. The stream on the left in the engine image appears to be under developed but, unfortunately, this is due a lack of illumination close to walls of the cylinder.

Although the environmental pressures are matched, temperatures are not as the engine work commences with a minimum cylinder head temperature of 65^0C. Nevertheless, these images show that at low engine speeds the air motion is unable to significantly disrupt the streams of the fuel spray; the inlet air momentum is weak compared to the spray momentum.

The first spray image in Figure 4.1 is at a time 0.33 ms or 1.4^0 CA later than the images in Figure 6. The central and far right streams have impacted on the piston crown

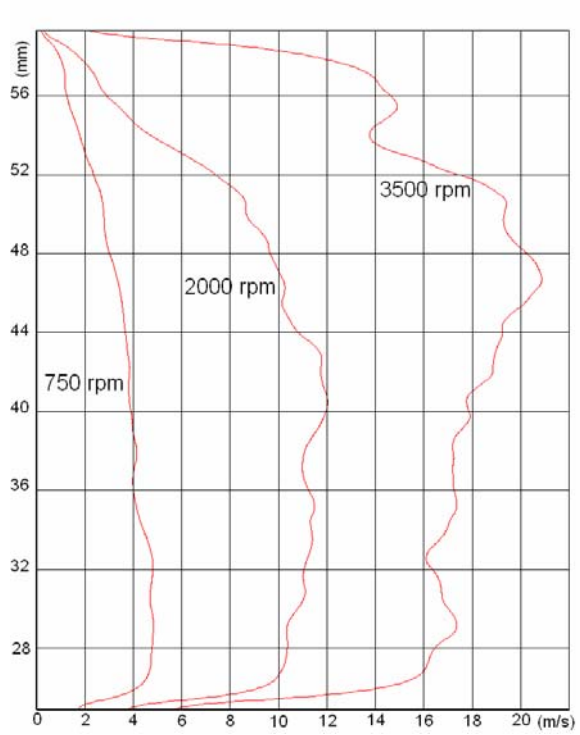

Crank angle - 120°

Fig. 5: Radial velocity component across cylinder axis

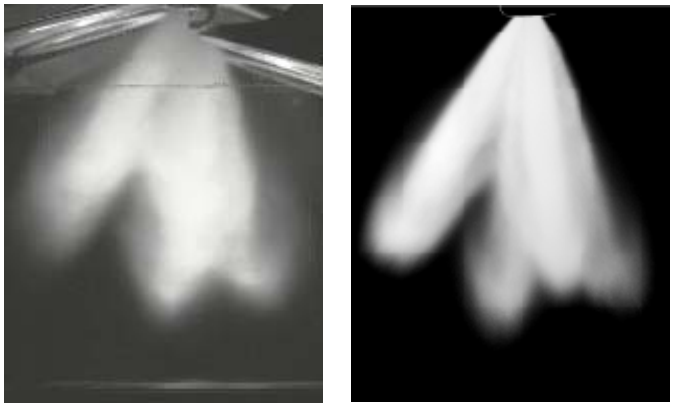
750rpm - Engine
1.0ms ASOI / 94.6° CA

Atmospheric spray bench
1.0ms ASOI

Fig. 6: Comparison of sprays under engine and atmospheric conditions

without any lateral displacement by the air flow. However, as the engine speed rises and the inlet airflow velocity increases then the spray images at 2000 and 3500 rpm in Figure 4.1 show significant disruption to the streaks. The near nozzle portion of the spray shows clearly that it is convected downstream with the air flow through the inlet valve gap. The downstream disruption is evident but at 108^0CA but there is still impact on the piston crown by the central stream. The spray at 120^0C has the highest cross flow on the cylinder line, Figure 5, yet this flow does not appear to transport the spray across the cylinder centre. Spray images at earlier times show that it is difficult to identify separate streams and the spray is confined entirely to the left half of the cylinder. However, the spray still impacts on the piston crown later at 140^0CA.

The concept, that it is the early airflow through the valve gap that has a more significant effect than the in-cylinder air motion, is confirmed by the spray images in Figures 4.2 and 4.3 where the injection timing is retarded to 120 and 150^0C respectively. The spray structure and momentum dominates at the 750 rpm where the separate streams are clearly visible and penetration is high. Whereas the central streams impact on the piston crown for the 120^0CA injection timing this is not the case for 150^0CA where impact occurs later at 159^0CA.

As the engine speeds and air flows increase the spray structures for the 120^0CA injection timing loose their coherence as the streams apparently tend to merge. Again there is little evidence to suggest that the spray is transported across the cylinder by the airflow shown in the PIV flow field. Impact of the streaks on the piston crown for 2000 and 3500 rpm for this injection timing occurs at 147^0CA and 174^0CA respectively.

For the injection timing of 150^0CA the spray structure shows distinct streams for all engine speeds even though there appears to be a lateral shift left in the near nozzle spray. Even with such a late injection timing the central streams still impact on the piston crown, 159, 177 and 199^0CA for engine speeds 750, 2000 and 3500 rpm respectively.

6. SUMMARY

Two complementary experiments, PIV flow field mapping and Mie spray imaging have been performed in an optical single cylinder engine with a near centrally mounted multi-stream gasoline direct injector. Engine speeds of 750, 2000 and 3500 rpm and injection timings of 90, 120 and 150^0CA ATDC have been chosen to evaluate how these two variables affect the mixing of the spray within the engine cylinder.

The tumble airflow structure is consistent with engine speed but obviously the momentum of the airflow increases. While the disruption of the spray streams does depend on engine speed there is little evidence that the tumble flow structure transports the spray across the cylinder. By far the most significant airflow-spray interaction is to be found in the near nozzle region with the high velocity flows through the inlet valve gap being responsible for disruption of the spray structure, particularly for early injection timings.

7. REFERENCES

1. Wigley, G., Garner, C., Stansfield, P., Pitcher, G., Turner, J., Nuglish, H., Air Fuel Mixing in a Homogeneous Direct Injection Spark Ignition Engine with a Fully Variable Valve Train System. Haus der Technik, 7th International congress – Engine Combustion Processes, Munich, March 15th -16th, 2005
2. Schwarz, CH., Schünemann, E., Durst, B., Fischer, J., Witt, A., Potentials of the Spray-Guided BMW DI Combustion System, SAE 2006-01-1265
3. Turner, J., Pearson, R. and Kenchington, S., Concepts for Improved Fuel Economy from Gasoline Engines, International Journal of Engine Research, Vol. 6, Number 2, April 2005, pp. 137-157(21).
4. Zhao, F., Harrington, D. and Lai, M., Automotive Gasoline Direct Injection Engines. SAE Publications, ISBN: 0768008824., 2002
5. Mariq, M.M., Podsiadlik, D.H., Brehob, D. D., and Haghgooie, M.; "Particulate Emissions from a Direct-Injection Spark-Ignition (DISI) Engine", SAE Technical Paper 1999-01-1527, 1999.
6. Salber, W., Wolters, P., Esch, T., Geiger, J. and Dilthey, J., Synergies of Variable Valve Actuation and Direct Injection. Society of Automotive Engineering, 2002-01-0706, 2002.
7. Sugiyama, M., Oil dilution reduction study with direct injection, Proceedings of Japanese Society of Automotive Engineering, 1997, JSAE, pp173-176, 1997.